CHAPTER VII
QUALITATIVE STUDIES OF SOLUBILIZATION AND ADSOLUBILIZATION OF ORGANIC SOLUTES BY DIFFERENTAIL SCANNING CALORIMETRY*

7.1 Abstract

This study examines solubilized and adsolubilized n-octane, p-tolunitrile, 4-bromotoluene, diphenylether and diphenylmethane using differential scanning calorimetry (DSC). Cetylpyridinium chloride (CPC), a cationic surfactant, was used to form micelles and admicelles capable of solubilizing the solutes from aqueous solution at pH 8. Admicelle formation was accomplished on precipitated silica as the solid substrate for surfactant adsorption. The data suggests the following: (1) CPC micellar and admicellar phases are liquid-like (2) there are three major loci of solubilization observed by DSC, i.e. the hydrated palisade/headgroup region, the non-hydrated palisade region and the core/solute drop region (3) for solubilization, with increasing total solute concentration it is possible for solute drops to form in micelles at low solute concentration which then disappear with increasing the solute concentration and possibly reappear in the micelle as solute concentration increases to sufficiently high values, (4) surfactant molecules in admicelles appear to pack more densely than the same surfactant molecules in micelles, and (5) DSC analysis can not differentiate between adsolubilized solutes residing in the non-hydrated and hydrated regions because the packing density of surfactant molecules in the admicelle may be uniform throughout the admicellar phase regardless of locus of adsolubilization. Subsequent adsolubilization makes admicelles more loosely packed with increasing solute concentration in the admicelles.

---

* Accepted by Colloid and Surfaces A 2007

7.2 Introduction

Surfactants in aqueous solution have the remarkable ability to self-assemble as three-dimensional aggregates, called micelles, when a critical micelle concentration (CMC) is reached [1]. A typical micelle at CMC is a roughly spherical or globular aggregate with the hydrophilic "head" regions in contact with the surrounding water, sequestering the hydrophobic tail regions in the micelle center. The micelle provides a microenvironment conductive to the partitioning of solute molecules which are otherwise sparingly soluble in the aqueous solution, a phenomenon known as solubilization [1-3]. When surfactant molecules are dispersed in an aqueous solution that also has a solid substrate, the surfactant molecules may aggregate as two-dimensional structures, called admicelles, which are somewhat similar in structure to micelles, at the solid/liquid interface [4]. The solubilization of solute by admicelles has been termed adsolubilization [4].

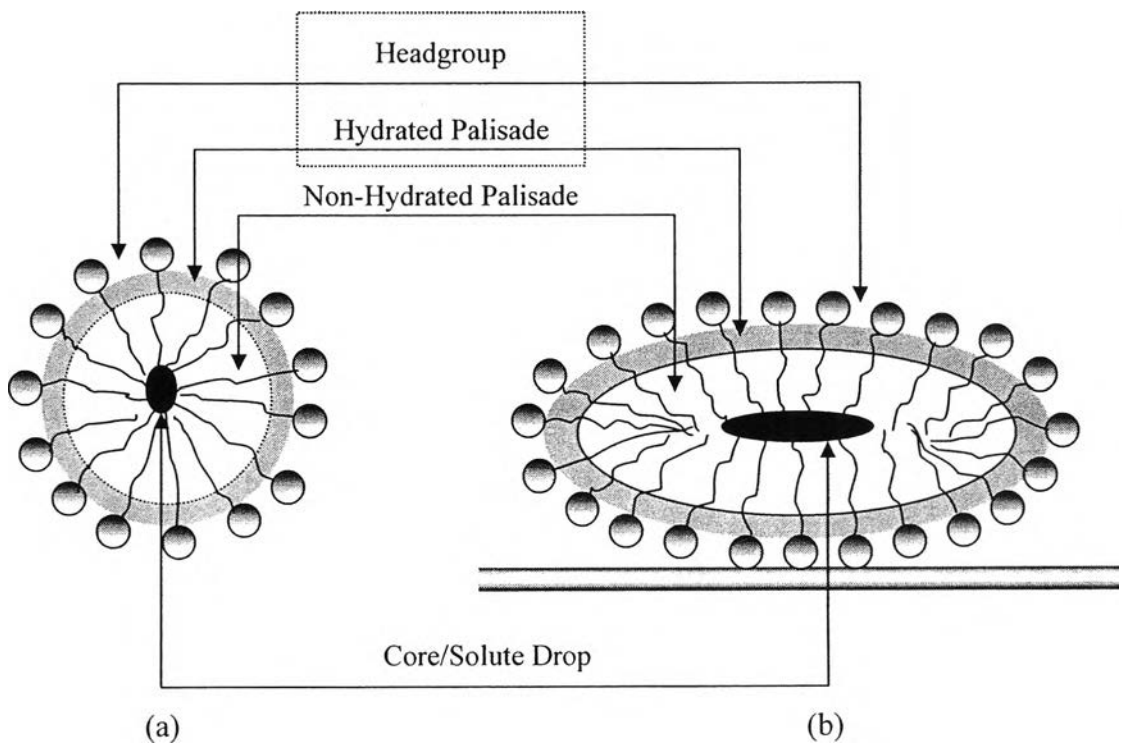

Figure 7.1 Typical micelle (a) and admicelle (b) structures with proposed loci of solubilization and adsolubilization.

Considering the wide number of applications of solubilization and adsolubilization [5-15], a clear knowledge of the nature of the surfactant aggregate interior has become very important. It is generally agreed that the primary locations for solubilization of neutral organic solutes in surfactant aggregates have been divided into three main parts by polarity [1, 16-17] (see Figure 7.1). These areas consist of the (1) headgroup region (2) hydrated palisade region and (3) non-hydrated palisade region. These proposed locations of various solutes solubilized in the surfactant aggregates have been elucidated by NMR spectroscopy [18-21].

The outer region is the most polar, consists of the surfactant headgroups, and forms the surfactant aggregate/water (and surfactant aggregate/solid for admicelle) interface. The inner region (surfactant tail region) is referred to as the palisade region. This region is divided into two sections based upon the presence of water. The first region is the hydrated palisade region which consists of the carbons near the headgroups and which is also characterized by water molecules that have penetrated the surfactant aggregates [22-24]. This region is intermediate in polarity. The second region, the non-hydrated palisade region, consists only of hydrocarbon chains and is nonpolar in nature [1]. Within the micelle, the palisade region consists of intertwined, randomly oriented hydrocarbon groups, forming a liquid-like region having a viscosity approximately an order of magnitude greater than that of liquid hydrocarbons of similar chain length [25]. The palisade region of the admicelle is similar but denser [4]. Sometimes, when micelles solubilize large amounts of highly hydrophobic solutes, the micelles tend to radially expand (swell) and pure solute droplets are then formed in the micelles [18, 26]. This phase separation can also happen with admicelles [27]. We propose an additional region, the core/solute drop region, as shown in Figure 7.1. Various studies have indicated that organic solutes partition into the regions of the surfactant aggregates that possess similar polarity [1-4, 28]. Thus, alkanes or other nonpolar solutes partition primarily to the non-hydrated palisade or core/solute drop region, while polar components partition to the hydrated palisade or headgroup region.

It has been suggested that the location of the solubilized/adsolubilized solutes can be determined by examining the graph of the partition coefficient plotted against the mole fraction of solute in the surfactant aggregates [3, 4, 6, 29, 30]. The

following trends have been proposed concerning the locus of solubilization and partition coefficients: (1) if the solute partitions primarily to the non-hydrated region (non-hydrated palisade or core/solute drop region), the partition coefficients will increase as solute mole fraction in the surfactant aggregates increases; (2) if the solute partitions primarily to the hydrated region (hydrated palisade or headgroup region), the partition coefficients will decrease as the solute mole fraction in the surfactant aggregates increases; and (3) if the solute partitions to both the hydrated and the nonhydrated regions, the partition coefficient will remain constant as solute mole fraction in the surfactant aggregates increases. It is possible that this data can roughly distinguish solute partitioning between solute in the hydrated region and solute in the non-hydrated regions of the micelle/admicelle.

In this study, we aim to elucidate the locus of solubilization/adsolubilization by determining the melting point variation of solute in the micelle/admicelle upon changing solutes type and their total concentrations at constant surfactant concentration. The study has been conducted by DSC and provides more detail about the micelle and admicelle interiors than those interpreted from the partition coefficient trend. The results mainly indicate that there are three clearly distinguishable sites for solubilization, whereas different sites for adsolubilization could not be distinguished due to an apparently uniform environment in the admicellar phase.

7.3 Materials and Methods

7.3.1 Materials

Precipitated silica powder, Hi-Sil® 233, with a specific surface area of 150 m^2/g was supplied by PPG Industries Inc. (Pittsburgh, PA) and used as a solid substrate. The cationic surfactant cetylpyridinium chloride (CPC) (99.8% in hydrated form) was obtained from Sigma (St. Louis, MO). The studied solutes include n-octane 99.5% (Fluka, St. Louis, MO), diphenylmethane 99+% (Aldrich, St. Louis, MO), diphenylether 99+% (Aldrich, St. Louis, MO), 4-bromotoluene (99+%) from Fluka (St. Lois, MO) and p-tolunitrile (98+%) from Fluka (St. Louis, MO). De-ionized water with a resistivity of 18.2 MΩ-cm was obtained from a Barnstead E-

pure water system. All chemicals were used as received. Physical properties of the studied solutes are shown in Table 7.1 [31].

Table 7.1 Physicochemical properties of the studied solutes.

Solutes	Chemical Formula	Aqueous Solubility at 25 °C (μmol/L)	Melting point (°C)	Boiling point (°C)
n-Octane	C_8H_{18}	5.78	-56.8	126
Diphenylmethane	$C_{13}H_{12}$	83.8	25.2	264
Diphenylether	$C_{12}H_{10}O$	106	26.8	259
4-Bromotoluene	C_7H_7Br	643	28.5	184
p-Tolunitrile	C_8H_7N	7860	29.5	217

7.3.2 Sample Preparation for DSC Analysis

We examined both the solubilization and adsolubilization of organic solutes by DSC. To prepare samples for DSC study of solubilization, we primarily assumed the critical micelle concentration of CPC to be 900 μmol/L [1]. A stock micellar solution of 5880 μmol/L (~6×CMC) was prepared and adjusted to pH 8. The CMC at pH 8 is also approximately 900 μmol/L [32], thus the concentration of micellar surfactant is around 4980 μmol/L. Twenty milliliters of this solution was mixed with a measured amount of the solute in a glass vial and then sealed. The solutions were equilibrated for two days prior to analyzing by DSC.

For adsolubilization study, a stock micellar solution was prepared for the same concentration of the micellar solution and the solution pH was adjusted to 8 using NaOH solution. The desired amount of solute was dissolved in 20 ml of the micellar solution in a glass vial, vigorously stirred and then sealed. After that, 0.4 g of silica powder was added to the solution. A bulk aqueous surfactant concentration at equilibrium after silica addition was just below the critical micelle concentration (~0.9×CMC). The surfactant molecules consequently self-assemble as admicelles at

silica/aqueous interface without a presence of micelles in the bulk aqueous phase. This system was equilibrated for two days prior to sampling to be analyzed by DSC.

7.3.3 Differential Scanning Calorimetry

DSC experiments were performed on Calorimetry Sciences Corporation (CSC) 6100 Nano II Differential Scanning Calorimeter, which is suitable for analysis of even small amount of solute in aqueous solution. The liquid sample and reference were each loaded into DSC cells (with nominal volume of 0.33 mL) in the cell chamber. The cell chamber was then tightly closed and pressurized to 4.5 atm. Before running the DSC, the stable heat transfer rate through those liquids must be lower than 30 μW as the pressure was increased from 0 to 3 atm to ensure that no small bubbles, which will significantly disturb solution properties leading to wrong DSC curve, are present in the cells. The sample and reference were equilibrated at the initial temperature (5°C) for 10 minutes. The DSC measures the heat transfer rate (μW) through the sample background-corrected by a corresponding reference. Heat transfer rate data were normally collected between 5 and 60 °C at a constant scan rate of 1 °C/min. However, only the temperature range between 5-30 °C in the DSC curve was presented in this paper because results above this range did not show any peaks. Our analysis on DSC curve is qualitatively based on the observed phase transition temperature. Only DSC heating curve was used to interpret the locus of solubilization and adsolubilization.

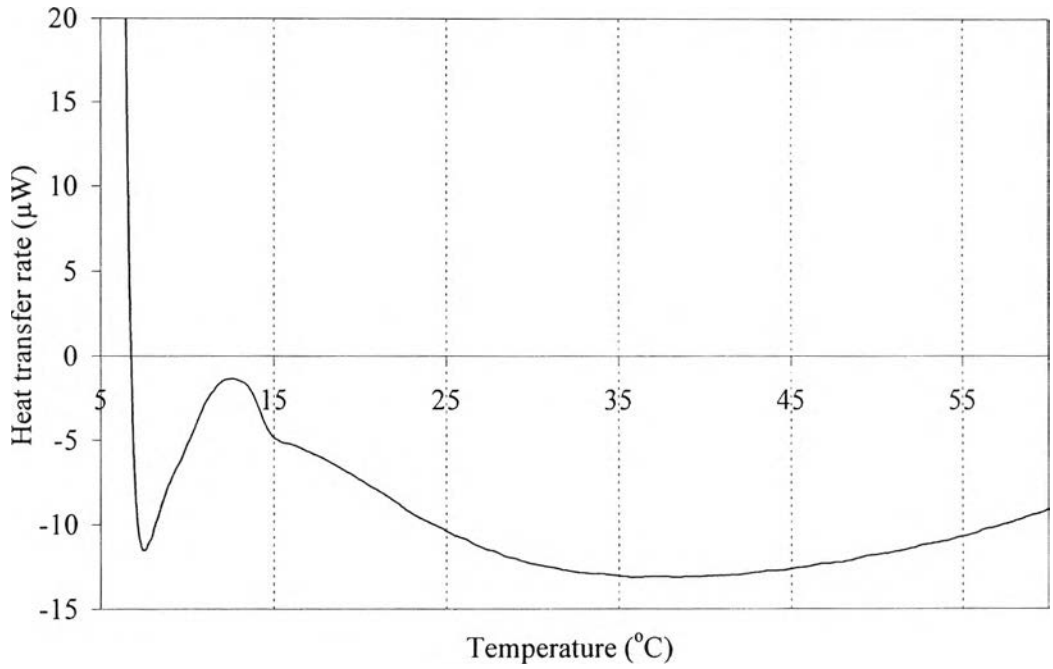

Figure 7.2 DSC heating curve of 5880 μmol/L CPC micellar solution (pH 8), which is background-corrected by de-ionized water.

7.4 Results and Discussion

7.4.1 Solubilization

Through the DSC analysis we expected to see some phase transitions / "melting points" for the solute in micelles. This process should be endothermic; forming a downward-pointing peak in the DSC heating curve. Figure 7.2 shows DSC curve as temperature dependence of the heat transfer rate through a 5880 μmol/L CPC micellar solutions (~6×CMC), which is background-corrected by de-ionized water. The temperature increases from 5°C, crosses the Kraft point of CPC (10±1°C at pH 8), and then up to 30°C. The DSC curve of this CPC solution is very similar to that of degassed/de-ionized water (not shown here). There is no significant endothermic peak presents in this DSC curve, not at the Kraft temperature nor at the melting point of CPC hydrocarbon chains (~19°C). It seems the micellar phase in the 5880 μmol/L CPC solution is liquid-like. This micellar solution was further used for our solubilization studies.

The solutes for our solubilization study are n-octane, p-tolunitrile, 4-bromotoluene, diphenylether and diphenylmethane, which are expected to be solubilized at different locations in the micelle. This study will use these neutral solutes as molecular probes to examine microenvironment in the micelle as analyzed from differential scanning calorimetric results.

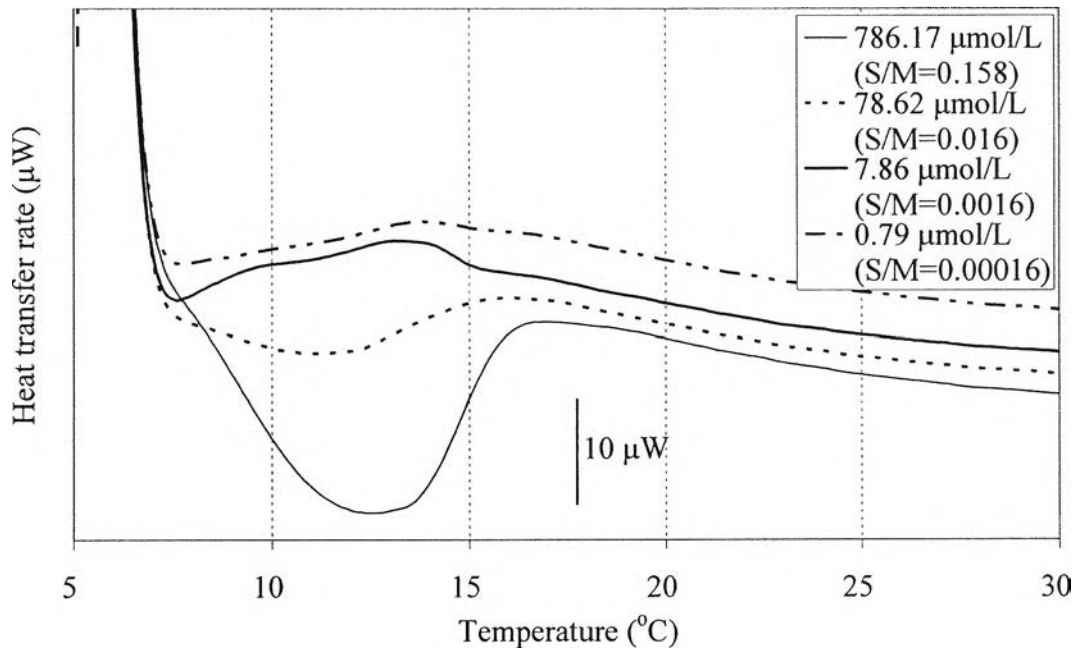

Figure 7.3 DSC heating curve of the p-tolunitrile-solubilized CPC (5880 μmol/L) micellar solutions (initial pH 8), which is background-corrected by the 5880 μmol/L CPC micellar solution (pH 8), at various total concentrations of p-tolunitrile. S/M is the ratio of total solute concentration / micellar surfactant concentration.

7.4.1.1 p-Tolunitrile Solubilization

p-Tolunitrile possesses high aqueous solubility (7861 μmol/L) and a melting point of 29.5°C. It has been previously shown that p-tolunitrile mainly solubilized in the hydrated region of admicelles [32]. We would expect it to partition into the same region in micelles. Figure 7.3 shows the DSC heating curve of the p-tolunitrile-solubilized CPC (5880 μmol/L) micellar solutions, which is background-corrected by the 5880 μmol/L CPC micellar solution, at various total concentrations

of p-tolunitrile. At very low p-tolunitrile concentration (0.79 μmol/L), the DSC curve exhibits no peaks, indicating that the solubilizing micelles are similar to the micelle without solubilized solute. This might be due to the very small amount of solubilized p-tolunitrile in the micelles. The initial development of the peak was observed around 10-13°C when the p-tolunitrile concentration was increased to 7.86 μmol/L. As p-tolunitrile concentration was increased to 78.62 μmol/L, The DSC curve clearly shows an endothermic peak (melting point) at 11.13°C, which we suggest as the melting point of p-tolunitrile solubilized in the micelle because (1) the pure micelles did not show any peak and (2) p-tolunitrile dissolved in water does not show any DSC peak at this temperature (not shown). This melting point is lower than that of pure p-tolunitrile (29.5°C). It means the mobility of p-tolunitrile in its pure phase is more restricted than that in the micelles (at hydrated region). This is also consistent with the loose packing of surfactant molecules near the micelle/solution interface. As the p-tolunitrile concentration was increased to 786.17 μmol/L, the peak location shifts to 12.6 °C. This shifting of the peak location to higher temperature with increasing p-tolunitrile concentration possibly implies that the location of subsequently solubilized p-tolunitrile molecules moves deeper into more densely packed non-hydrated region of the micelle. This is consistent with the data collected for the adsolubilization of this solute, that is, the p-tolunitrile partition coefficient decreases with increasing intra-admicelle mole fraction at low intra-admicellar mole fraction and (2) the partition coefficient becomes nearly constant and then gradually increases upon increasing intra-admicellar mole fraction at intermediate and high intra-admicellar mole fractions [32].

7.4.1.2 n-Octane Solubilization

n-Octane is nonpolar and presumably solubilizes into the non-hydrated palisade region of the micelle [3, 30] without swelling the micelle [33-37]. Figure 7.4 shows the DSC heating curve of n-octane-solubilized CPC (5880 μmol/L) micellar solutions, background-corrected by a 5880 μmol/L CPC micellar solution, at various total concentrations of n-octane. It was shown that a low total concentration of n-octane (615 μmol/L) in the micellar solution did not exhibit any peak on DSC curve, which might be due to too small solubilized n-octane in the micelles. When the total concentration of n-octane was increased to 1846 μmol/L, DSC curve shows

an endothermic peak (melting point) at 11.7 °C. This melting point is supposed to be that of the solubilized n-octane in the micellar phase - pure micellar solution and completely dissolved n-octane in water did not show any peak on DSC curve. This peak is much higher than that of pure n-octane (-56.8 °C). The appearance of this higher melting point indicates that the mobility of solubilized n-octane molecules in the micelles are much more restricted than those in its pure phase. As the total concentration of n-octane in the micellar solution was increased to 4308 μmol/L, the peak observed in the DSC curve slightly shifts to higher temperature, again suggesting that n-octane begin solubilizing deeper into the more densely packed non-hydrated region of the micelle, much the same as with p-tolunitrile.

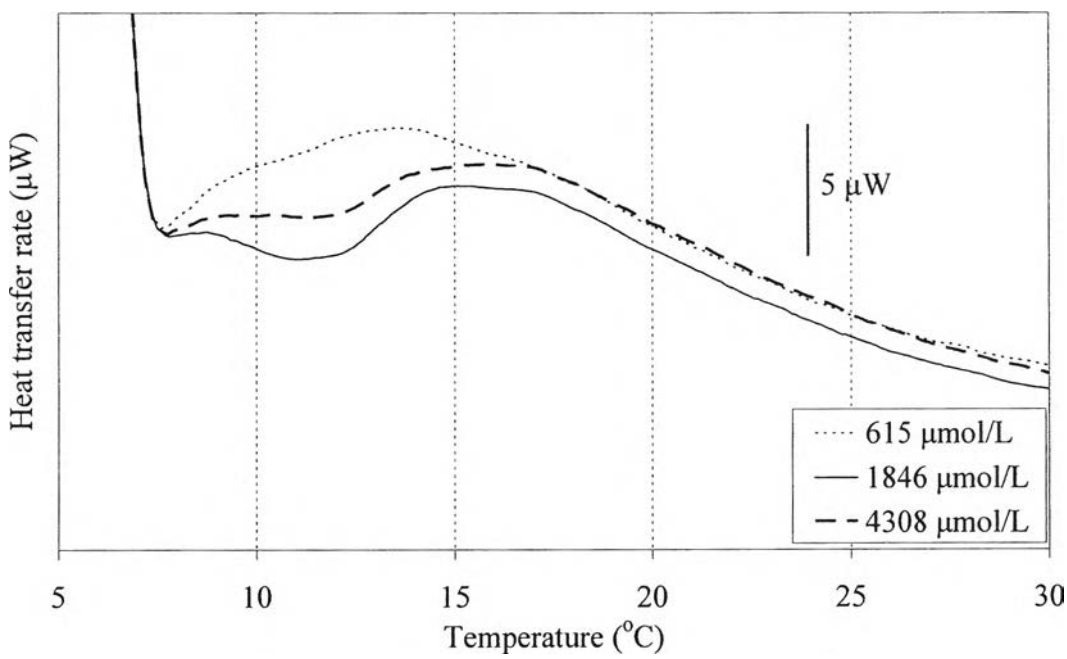

Figure 7.4 DSC heating curve of n-octane-solubilized CPC (5880 μmol/L) micellar solutions (initial pH 8), which is background-corrected by a 5880 μmol/L CPC micellar solution (pH 8), at various total concentrations of n-octane.

Comparing n-octane and p-tolunitrile in the micelle, the phase transition temperature of n-octane is slightly lower than that of p-tolunitrile. This suggests that the mobility of p-tolunitrile located in the hydrated region is more

restricted than n-octane located in the non-hydrated region of the micelle, even though the non-hydrated region is basically denser. We suggest two reasons for this. First, the effects of cation-π binding and dipole-dipole attractive interactions in the vicinity of the CPC headgroups near the micelle/water interface plays a vital role for p-tolunitrile. These attractive interactions are normally stronger than hydrophobic forces, which exist for n-octane. Second, attractive forces between n-hexane and n-alkyl surfactant tails in the micelle is most likely weaker than the attractive force between p-tolunitrile and the tails. This is suggested by the much lower values of both melting and boiling points (indicating weaker cohesive force [38]) of n-octane. We found that different solutes solubilized in different regions in the micelles did not always show clearly different molecular mobility as represented in the DSC curve. Thus, DSC does not appear able to distinguish the difference in the location of solutes in these studied cases (p-tolunitrile and n-octane). To validate the DSCs ability to analyze solute location in the micelles, we have to minimize effect from the second reason above and consequently examine the other solutes (instead of n-octane) possessing melting points and/or boiling points that are similar to p-tolunitrile (see Table 7.1), such as 4-bromotoluene, diphenylether and diphenylmethane. These solutes have polarities decreasing in the order of p-tolunitrile > 4-bromotoluene > diphenylether > diphenylmethane.

7.4.1.3 4-Bromotoluene Solubilization

4-Bromotoluene has a low aqueous solubility (643 μmol/L) and a melting point of 28.5°C. Figure 7.5 shows the DSC heating curve of 4-bromotoluene-solubilized CPC (5880 μmol/L) micellar solutions, background-corrected by the 5880 μmol/L CPC micellar solution, at various total concentrations of 4-bromotoluene. The 4-bromotoluene concentration of 0.64 μmol/L DSC curve exhibits two peaks. The first peak is located at ~12.0°C, whereas the second peak is located at ~15.7°C, which may be the phase transition points of 4-bromotoluene residing in the sharply different environments. Both peak locations are nearly unchanged with increasing concentration of 4-bromotoluene from 0.64 to 6.43 to 64.31 to 643.12 μmol/L, suggesting that the phase transition point of 4-bromotoluene in the micelle is concentration-insensitive.

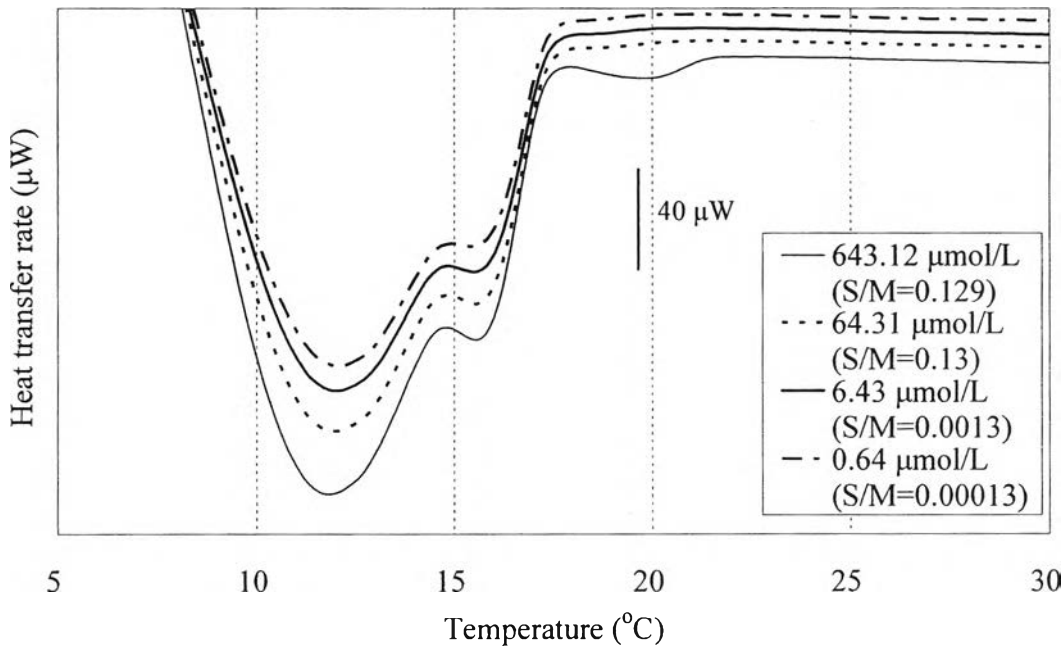

Figure 7.5 DSC heating curve of the 4-bromotoluene-solubilized CPC (5880 μmol/L) micellar solutions (initial pH 8), which is background-corrected by the 5880 μmol/L CPC micellar solution (pH 8), at various total concentrations of 4-bromotoluene.

Additionally, if the concentration of 4-bromotoluene is very high (643.12 μmol/L, its aqueous solubility), an additional peak appears at around 20°C. Thus, there are three transition points (at ~12, ~16 and ~20 °C) of 4-bromotoluene solubilized in the micelles. We believed those three transition points correspond to three different locus of solubilization. To identify them, we consider the sharply different nature of the possible loci, (1) core/solute drop region in the micelle (2) densely/non-hydrated palisade region and (3) loosely/hydrated region (hydrated palisade/headgroup) as similarly interpreted from NMR spectroscopic results for benzene solubilization [18]. The first locus is confirmed by solubilized p-tolunitrile which gives the same peak location at 12 °C (in section *7.4.1.1.*). Therefore, in the case of 4-bromotoluene, the transition points of 12, 16 and 20 °C should corresponds to solute residing in the hydrated palisade/headgroup, non-hydrated palisade and core/solute drop regions of the micelles, respectively.

7.4.1.4 Diphenylether Solubilization

Diphenylether has an aqueous solubility of 106 μmol/L and a melting point of 26.8 °C, comparable with those 4-bromotoluene and p-tolunitrile. Figure 7.6 shows the DSC heating curve of the diphenylether-solubilized CPC (5880 μmol/L) micellar solutions, which is background-corrected by the 5880 μmol/L CPC micellar solution, at various total concentrations of diphenylether.

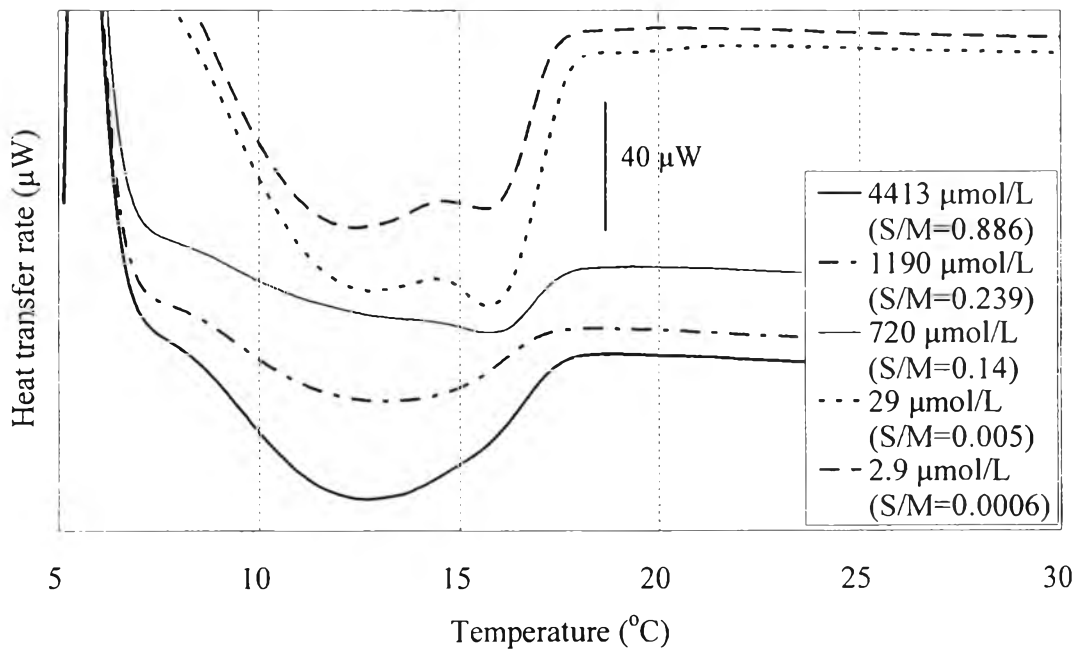

Figure 7.6 DSC heating curve of the diphenylether-solubilized CPC (5880 μmol/L) micellar solutions (initial pH 8), which is background-corrected by the 5880 μmol/L CPC micellar solution (pH 8), at various total concentrations of diphenylether.

At very low total concentration of diphenylether (2.9 μmol/L), the DSC curve shows the endothermic peaks at 12.4 and 15.8 °C. This may be compared with the peaks of 4-bromotoluene, which we suggest corresponding to diphenylether solubilized in the hydrated palisade/headgroup and the non-hydrated palisade regions of the micelles, respectively. The peak at 12.4 °C became more dominant when diphenylether concentration increased. In addition, both peaks tend to merge together to one peak at the around 12 °C (first peak) with increasing

diphenylether concentration. These indicate that the location of the subsequently-solubilized diphenylether molecules tends to move toward the aqueous phase. It was also observed that the merged peak smoothly covers the temperature range of the second peak. This implies that solubilization makes the sharp boundary between non-hydrated palisade region and hydrated palisade/headgroup region gradually merged possibly by making the non-hydrated palisade less densely packed (more disordered) with increasing diphenylether concentration.

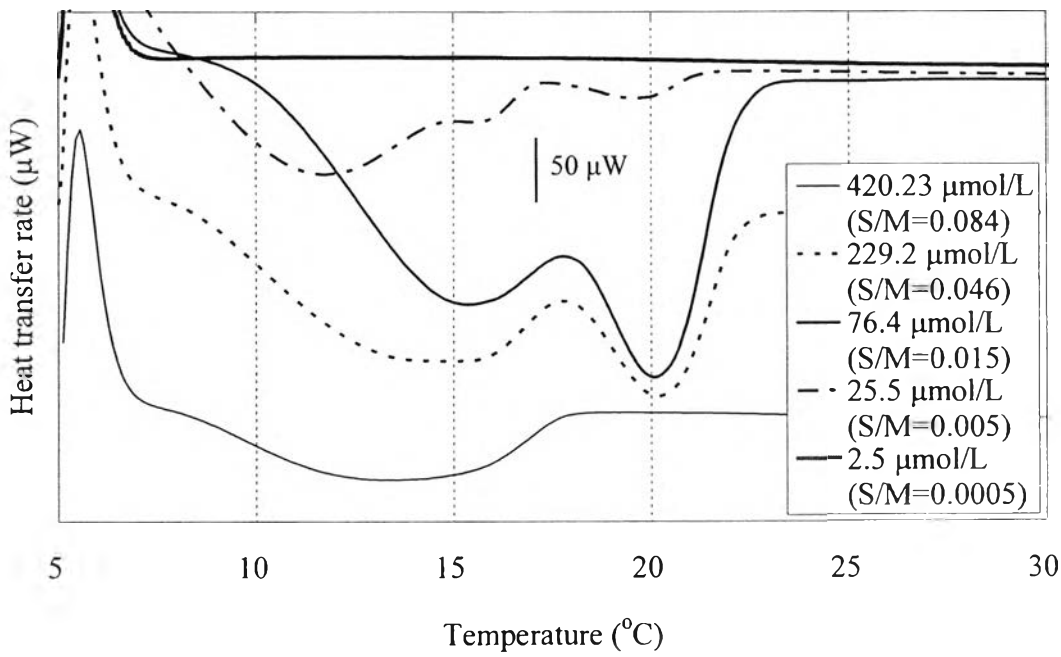

Figure 7.7 DSC heating curve of the diphenylmethane-solubilized CPC (5880 μmol/L) micellar solutions (initial pH 8), which is background-corrected by the 5880 μmol/L CPC micellar solution (pH 8), at various total concentrations of diphenylmethane.

7.4.1.4 Diphenylmethane Solubilization

Diphenylmethane possesses very low aqueous solubility (83.8 μmol/L), is weakly polarizable, and has a melting point of 25.2 °C, close to that of diphenylether. Figure 7.7 shows the DSC heating curve of the diphenylmethane-solubilized CPC (5880 μmol/L) micellar solutions, which is background-corrected by

the 5880 μmol/L CPC micellar solution, at various total concentrations of diphenylmethane. At very low diphenylmethane concentration (2.5 μmol/L), the DSC curve show no peaks. Different from 4-bromotoluene, when the total concentration of diphenylmethane was increased to 25.5 μmol/L, the DSC curve shows three peaks (transition points) at ~12, ~16 and ~20 °C, even at this very low concentration. As similar peak locations were observed for solubilized 4-bromotoluene, they should correspond to solute located in the hydrated palisade/headgroup, non-hydrated palisade and core/solute drop regions, respectively. When the diphenylmethane concentration was increased to 76.4 μmol/L, the first peak at 12°C disappears suggesting that solubilized diphenylmethane moves deeper into the micellar interior. Above a diphenylmethane concentration of 229.2 μmol/L, the second peak at around 16 °C shifts to a lower temperature (13.4 °C) and the third peak at 20 °C disappears. The location of this peak is between that of the initial first and second peaks. Moreover, this peak area does not cover the range of the former third peak. These mean at high diphenylmethane concentration, the core/solute drop region formation is not preferred. Diphenylmethane is totally solubilized at the merged non-hydrated palisade and hydrated palisade/headgroup regions. The property of this merged region should be somewhat of an average between those two regions.

7.4.2 Adsolubilization

Adsolubilization was studied by using a 5880 μmol/L CPC micellar solution mixed with amorphous silica to form admicelles in this mixture. This total surfactant concentration corresponds to admicellar surfactant concentration of 5480 μmol/L [32] This case, the bulk aqueous concentration of CPC was just below the CMC. Figure 7.8 shows the DSC heating curve of a 5880 μmol/L CPC micellar solution (pH 8) mixed with silica powder to form admicelles, which is background-corrected by silica/water mixture. It is very similar to the curve obtained from degassed/de-ionized water and the micellar solution (not shown). This suggests that the admicellar phase is still liquid-like. This admicellar solution will be used for all adsolubilization studies.

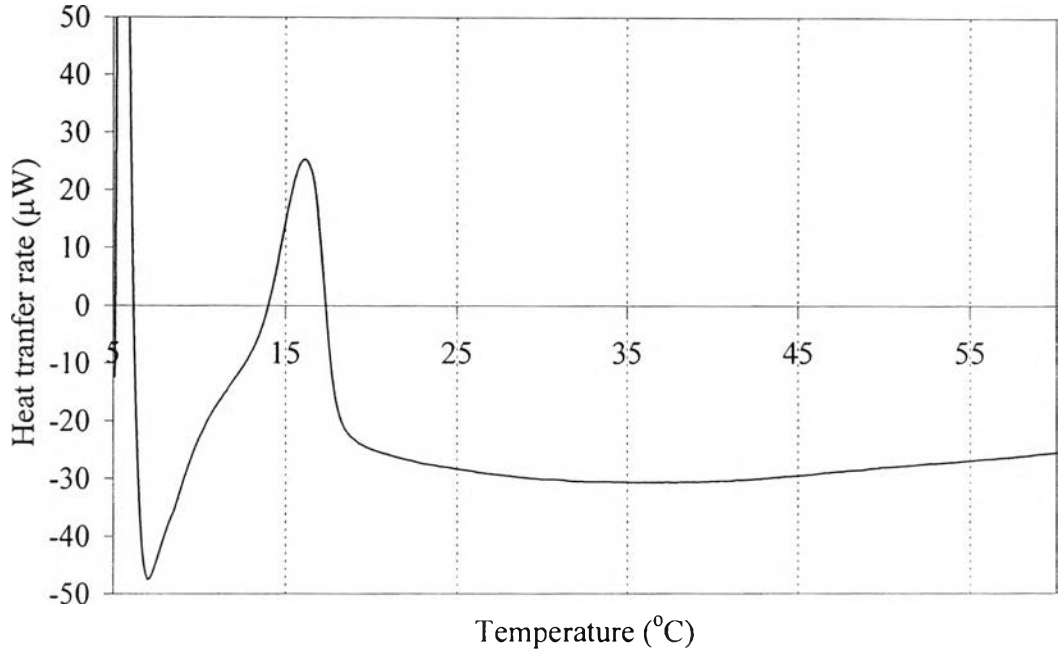

Figure 7.8 DSC heating curve of a 5880 μmol/L CPC micellar solution (pH 8) mixed with silica powder to form admicelles, which is background-corrected by silica/water mixture.

7.4.2.1 p-Tolunitrile Adsolubilization

Figure 7.9 shows the DSC heating curve of p-tolunitrile-adsolubilized CPC (5880 μmol/L) admicellar solutions mixed with amorphous silica, which is background-corrected by the 5880 μmol/L CPC admicellar solution mixed with silica, at various total concentrations of p-tolunitrile. At a p-tolunitrile concentration of 26.21 μmol/L, the DSC curve presents only one peak at 16.9 °C. This peak position shifts to lower temperature upon increasing p-tolunitrile concentration. The peak is at 16.0 °C when the p-tolunitrile concentration reaches its aqueous solubility (7862 μmol/L). We initially thought that these peaks were in the vicinity of the second peak for solubiization, corresponding to solute residing in the non-hydrated palisade region of micelles. However, the adsolubilization results of p-tolunitrile interpreted from partition coefficient trends from the same system [32] implies that p-tolunitrile is mainly adsolubilized at the hydrated palisade/headgroup region of the admicelles. We will examine this conflict data later in this paper.

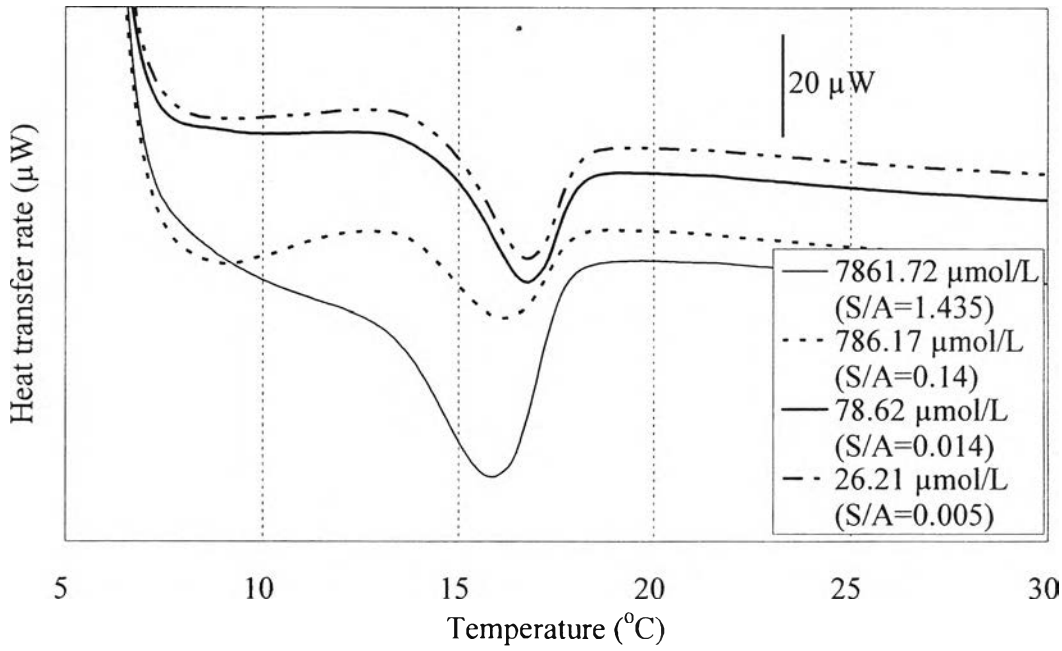

Figure 7.9 DSC heating curve of p-tolunitrile-adsolubilized CPC (5880 μmol/L) admicellar solutions (initial pH 8) mixed with silica powder, which is background-corrected by the 5880 μmol/L CPC admicellar solution (pH 8) mixed with silica powder, at various total concentrations of p-tolunitrile. S/A is the ratio of total solute concentration / admicellar surfactant concentration.

7.4.2.2 4-Bromotoluene/Diphenylether/Diphenylmethane Adsolubilization

The results from the adsolubilization of 4-bromotoluene, diphenylether and diphenylmethane interpreted from their partition coefficient trends imply that they are dominantly adsolubilized at the non-hydrated palisade region of the admicelles [32]. Figure 7.10, 7.11 and 7.12 shows the DSC heating curve of 5880 μmol/L CPC admicellar solutions (initial pH 8) mixed with silica and solubilizing 4-bromotoluene, diphenylether and diphenylmethane, respectively. The curve was background-corrected by the 5880 μmol/L CPC admicellar solution mixed with silica. All three systems gave similar results with only one DSC peak located at roughly 16 °C for all studied solute concentrations. The peak position and pattern are nearly the same as that observed from p-tolunitrile adsolubilization system, even

though the preferred location of these solutes in the admicelle is different from that of p-tolunitrile. This evidence solves the conflict on the preferred locus of adsolubilization of p-tolunitrile in the previous section. It suggests that the surfactant packing density and molecular interactions in the admicellar phase are rather uniform throughout the whole region of the admicelle corresponding to typical closely-packed bilayer structure/geometry of admicelles. This admicelle interior should be similar with the non-hydrated region of the micelles mentioned in the previous section. As with p-tolunitrile, this peak position still shifts to lower temperature upon increasing total solute concentration. However, it does not always mean these solute molecules are subsequently adsolubilized toward the aqueous phase; instead, it tells us that the interior of the admicelles become less compact with increasing solute amount in the admicelles. Different solute locations in the admicelles could not be distinguished by this DSC analysis.

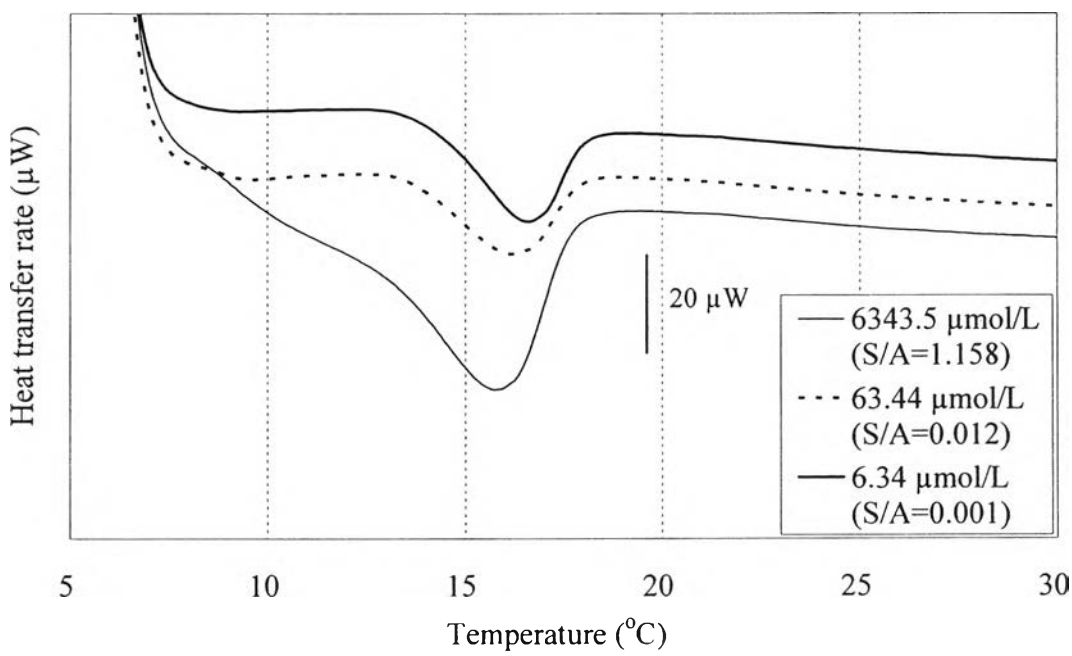

Figure 7.10 DSC heating curve of 4-bromotoluene-adsolubilized CPC (5880 μmol/L) admicellar solutions (initial pH 8) mixed with silica powder, which is background-corrected by the 5880 μmol/L CPC admicellar solution (pH 8) mixed with silica powder, at various total concentrations of 4-bromotoluene.

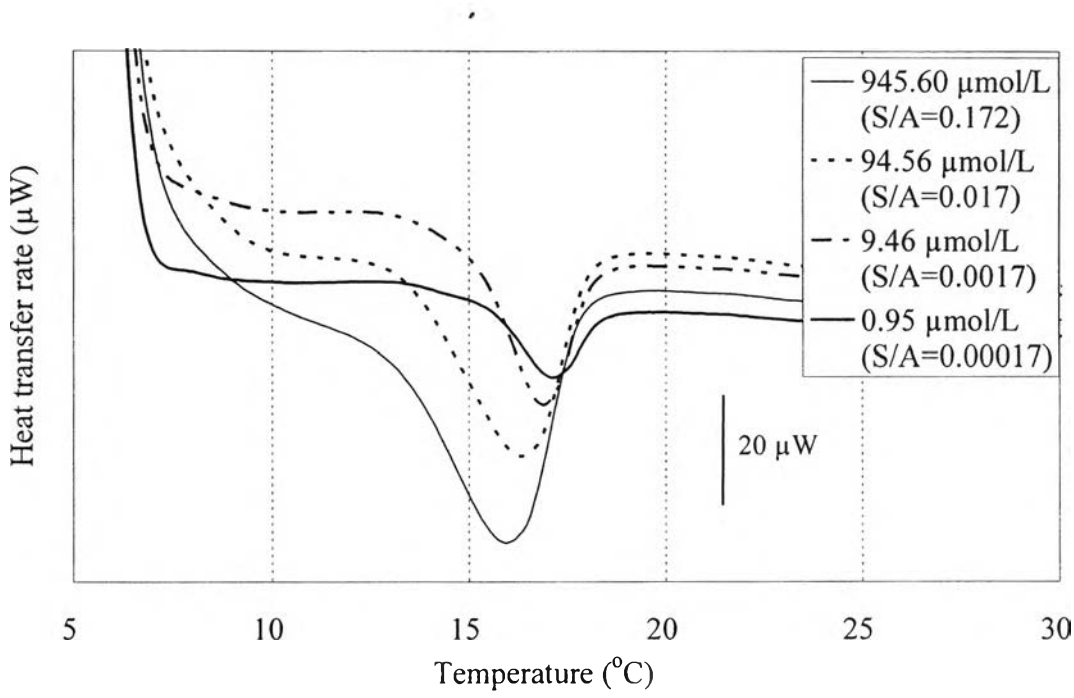

Figure 7.11 DSC heating curve of diphenylether-adsolubilized CPC (5880 μmol/L) admicellar solutions (initial pH 8) mixed with silica powder, which is background-corrected by the 5880 μmol/L CPC admicellar solution (pH 8) mixed with silica powder, at various total concentrations of diphenylether.

7.4.2.3 n-Octane Adsolubilization

Figure 7.13 shows the DSC heating curve of n-octane-adsolubilized CPC (5880 μmol/L) admicellar solutions mixed with silica, background-corrected by the 5880 μmol/L CPC admicellar solution mixed with silica, at various total concentrations of n-octane. It was found that only one peak was present (at 16.5 °C) at very low n-octane concentration (1.2 μmol/L). This concentration is very much lower than that which gave a clear DSC peak for the solubilization of n-octane. This suggests that surfactant molecules incorporated in admicelles pack more densely than those in micelles. This conclusion is also confirmed by higher value of this transition temperature (16.5°C) than that observed for n-octane solubilization (12°C). Additionally, the position of this peak moves to lower temperature upon increasing the n-octane concentration representing that the subsequently adsolubilized n-octane molecules also make admicelle less compact.

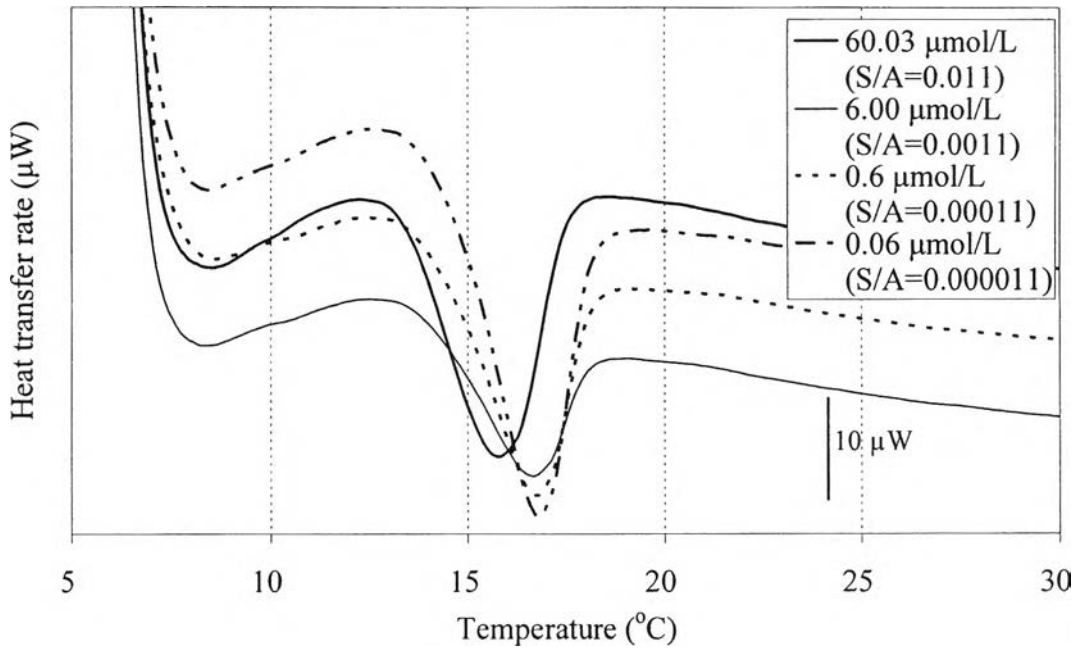

Figure 7.12 DSC heating curve of diphenylmethane-adsolubilized CPC (5880 μmol/L) admicellar solutions (initial pH 8) mixed with silica powder, which is background-corrected by the 5880 μmol/L CPC admicellar solution (pH 8) mixed with silica powder, at various total concentrations of diphenylmethane.

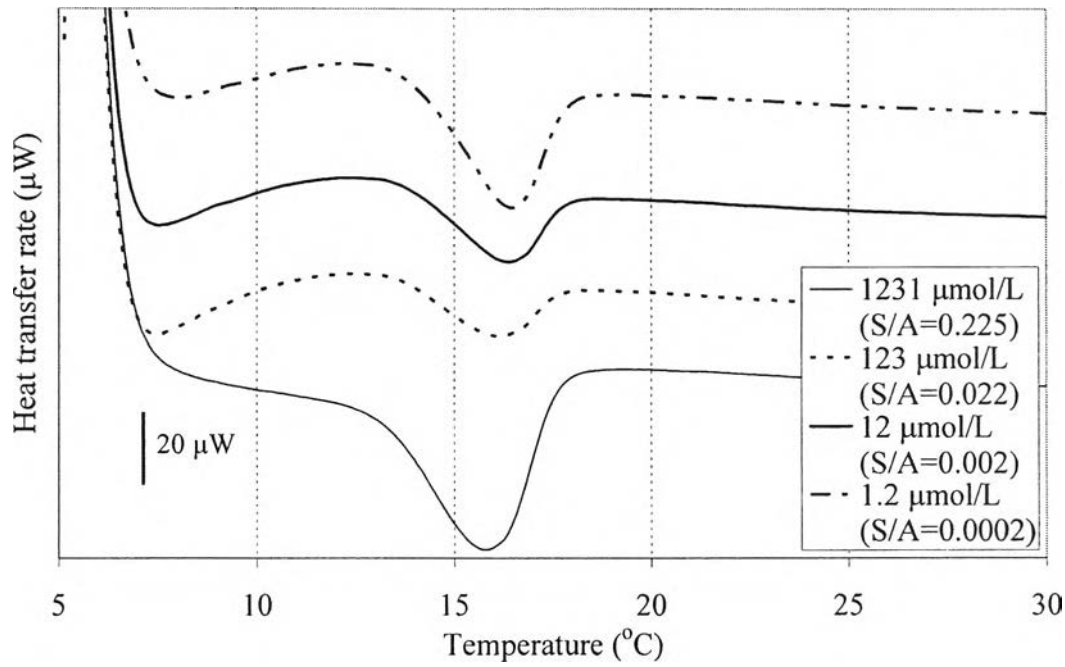

Figure 7.13 DSC heating curve of n-octane-adsolubilized CPC (5880 μmol/L) admicellar solutions (initial pH 8) mixed with silica powder, which is background-corrected by the 5880 μmol/L CPC admicellar solution (pH 8) mixed with silica powder, at various total concentrations of n-octane.

7.5 Conclusions

Based on the information obtained from the study of solubilization and adsolubilization of n-octane, p-tolunitrile, 4-bromotoluene, diphenylether and diphenylmethane by DSC, it was concluded that:

- CPC micellar and admicellar phases are liquid-like (low density, no DSC peak)
- There are three potential loci of solubilization observed by DSC: hydrated palisade/headgroup region, non-hydrated palisade region and core/solute drop region
- For solubilization, upon increasing total solute concentration it is possible for both (1) the formation of core/solute drop region in micelle initially occurs at low solute concentrations and then disappears upon

increasing solute concentration and (2) the core/solute drop region begin forming in micelles as the solute concentration is increased to high enough levels.

- Surfactant molecules in the admicelles appear to pack more densely than the same surfactant molecules in micelles.
- The DSC analysis can not distinguish between adsolubilization in the non-hydrated and hydrated regions because the packing density of surfactant molecules in the admicelle is possibly rather uniform throughout the whole region of admicellar phase regardless of locus of adsolubilization. Subsequent adsolubilization makes admicelles less compact upon increasing solute amount in the admicelles.

7.6 Acknowledgements

We are grateful to the Thailand Research Fund (TRF) for financial support through the Royal Golden Jubilee Ph.D. Program (Grant No. PHD/0217/2544). We also gratefully thank Assist. Prof. Susan Pedigo (Department of Chemistry and Biochemistry, The University of Mississippi) for useful suggestions on nano-DSC methodology and analysis.

7.7 References

[1] M.J. Rosen, Surfactant and Interfacial Phenomena, third eds., John Wiley & Sons, New York, 2004.

[2] R. Nagarajan, Current Opinion in Colloid Interf. Sci. 1 (1996) 391.

[3] C.S. Dunaway, S.D. Christian, J.F. Scamehorn, in: S.D. Christian, J.F. Scamehorn (Eds.), Solubilization in Surfactant Aggregates, Marcel Dekker, New York, 1995, pp. 3-31.

[4] J.H. O'Haver, J.H. Harwell, L.L. Lobban, E.A. O'Rear, in: S.D. Christian, J.F. Scamehorn, (Eds), Solubilization in Surfactant Aggregates, Marcel Dekker, New York, 1995, pp. 277-295.

[5] S.P. Nayyar, D.A. Sabatini, J.H. Harwell, Environ. Sci. Technol. 28 (1994) 1874-1881.

[6] T. Pradubmook, J.H. O'Haver, P. Malakul, J.H. Harwell, Colloid Surf. A 224 (2003) 93-98.

[7] G.P. Funkhouser, M.P. Arevalo, D.T. Glatzhofer, E.A. O'Rear, E.A., Langmuir 11 (1995) 1443-1447.

[8] W.L. Yuan, E.A. O'Rear, B.P. Grady, D.T. Glatzhofer, Langmuir 18 (2002) 3343-3351.

[9] K. Esumi, N. Watanabe, K. Meguro, Langmuir 7 (1991) 1775-1778.

[10] J.H. O'Haver, J.H. Harwell, E.A. O'Rear, W.H. Waddell, L.J. Snodgrass, Langmuir 10 (1994) 2588-2593.

[11] W.H. Waddell, J.H. O'Haver, L.R. Evans, J.H. Harwell, J.Appl. Polym. Sci. 55 (1995) 1627-1641.

[12] V. Thammathadanukul, J.H. O'Haver, J.H. Harwell, S. Osuwan, N. Na-Ranong, W.H. Waddell, J. Appl. Polym. Sci. 59 (1996) 1741-1750.

[13] J.H. O'Haver, J.H. Harwell, L.R. Evans, W.H. Waddell, J. Appl. Polym. Sci. 59 (1996) 1427-1435.

[14] K. Hayakawa, Y. Mouri, T. Maeda, I. Satake, M. Sato, Colloid Polym. Sci. 278 (2000) 553-558.

[15] C.T. Jafvert, Environ. Sci. Technol. 25 (1991) 1039-1045.

[16] M. Aamodt, M. Landgren, B. Jonsson, J. Phys. Chem. 96 (1992) 945-950.

[17] J. Dickson, J.H. O'Haver, Langmuir 18 (2002) 9171-9176.

[18] N. Hedin, R. Sitnikov, I. Furó, U. Henriksson, O. Regev, J. Phys. Chem. B. 103 (1999) 9631-9639.

[19] J.P. Mata, V.K. Aswal, P.A. Hassan, P. Bahadur, J. Colloid Interf. Sci. 299 (2006) 910-915.

[20] G. Lindblom, B. Lindman, L. Mandell, J. Colloid Interf. Sci. 42 (1973) 400-409.

[21] M.S. Goldenberg, L.A. Bruno, E.L. Rennwantz, J. Colloid Interf. Sci. 158 (1993) 351-363.

[22] H. Wennerstroem, B. Lindman, J. Phys. Chem. 83 (1979) 2931-2932.

[23] L.P. Novaki, O.A. El Seoud, Langmuir 16 (2000) 35-41.

[24] C.D. Bruce, S. Senapati, M.L. Berkowitz, L. Perera, M.D.E. Forbes, J. Phys. Chem. B. 106 (2002) 10902-10907.

[25] R. Zana, Surfactant Solutions: New Methods of Investigation, Marcel Dekker, New York, 1986.

[26] Y. Doi, Y. Kawashima, K. Matsuoka, Y. Moroi, J. Phys. Chem. B. 108 (2004) 2594-2599.

[27] C.H. See, J.H. O'Haver, Colloid Surf. A 243 (2004) 169-183.

[28] J.P. Mata, V.K. Aswal, P.A. Hassan, P. Bahadur, J. Colloid Interf. Sci. 299 (2006) 910-915.

[29] B. Kittiyanan, J.H. O'Haver, J.H. Harwell, S. Osuwan, Langmuir, 12 (1996) 2162-2168.

[30] J.H. O'Haver, J.H. Harwell, in: R. Sharma (Ed.), Surfactant Adsorption and Surface Solubilization, American Chemical Society, Washington, DC, 1995, pp. 49-66.

[31] Yaws, C.L., Ed., Chemical Properties Handbook, McGraw-Hill, New York, 1999.

[32] W. Saphanuchart, C. Saiwan, J.H. O'Haver, submitted to Colloid Surf. A. 2007

[33] D.Attwood, A.T. Florence, Surfactant Systems: Their Chemistry, Pharmacy, and Biology, Chapman and Hall, London, 1983.

[34] P.M. Lindemuth, G.L.Bertrand, J. Phys. Chem. 97 (1993) 7769-7773.

[35] R. Friman, J.B. Rosenholm, Colloid Polym. Sci. 260 (1982) 545-551.

[36] M.Almgren, S. Swarup, J. Phys. Chem. 86 (1983) 4212-4216.

[37] A. Malliaris, J. Phys. Chem. 91 (1987) 6511-6515.

[38] A.F.M. Barton, Ed., CRC Handbook of Solubility Parameters and Other Cohesion Parameters, second eds., CRC Press, New York, 1991.